

## Photoinduced Electrochemical Reduction of Nitrite at an Electrochemically Roughened Silver Surface

Junwei Zheng,<sup>†</sup> Tianhong Lu,<sup>‡</sup> Therese M. Cotton,<sup>†</sup> and George Chumanov\*,<sup>†</sup>

Department of Chemistry, Iowa State University, Ames, Iowa 50011, and Changchun Institute of Applied Chemistry, Chinese Academy of Sciences, Changchun, 130023, P. R. China

Received: March 17, 1999; In Final Form: May 24, 1999

Photoelectrochemical reduction of nitrite and nitrate was studied on the surface of an electrochemically roughened silver electrode. The dependence of the photocurrent on photon energy, applied potential, and concentration of nitrite was determined. It was concluded that the photoelectrochemical reduction proceeds via a photoemission process followed by the capture of hydrated electrons by electron acceptors. The excitation of plasmon resonances in nanosize metal structures produced during the roughening procedure resulted in the enhancement of the photoemission process. Ammonia was detected as one of the final products in this reaction. Mechanisms for the photoelectrochemical reduction of nitrite and nitrate are proposed.

### Introduction

The reduction of nitrite is of significant importance for many reasons including remediation of environmental pollutants and chemical technology. Nitrites are present in high concentration in caustic radioactive waste from nuclear plants, and the reduction to gaseous products would greatly lessen the volume of such waste.<sup>1,2</sup> The reduction of nitrite to various compounds (for example, hydroxylamine) would provide industrially useful intermediates for the production of many chemicals.<sup>3</sup> Methods based on electrochemical reduction can also be potentially used for the detection of nitrite in different analytical applications.<sup>4,5</sup>

Despite considerable effort, efficient electrochemical reduction of nitrite could not be achieved because of the large overpotential that is required at neutral and alkaline pH's (ca.  $-1.4$  V in 1 M NaOH at a Ag cathode<sup>6</sup>). The reduction can occur at less negative potentials in acidic media; however, under these conditions, nitrite is unstable and decomposes to form different species, thereby complicating the process.<sup>7</sup> Various approaches that have yielded some measure of success in lowering the high overpotential include the use of catalytic electrode materials, such as Ni,<sup>6</sup> Zn,<sup>6</sup> Cd,<sup>8</sup> and Cu,<sup>6</sup> the addition of catalysts such as metal cyclams to the electrolytic solution,<sup>9</sup> and the adsorption of the catalyst on the electrode, as in the case of copper–phenanthroline complexes on graphite.<sup>10</sup> Highly promising photoassisted reduction of nitrate has been also studied at mercury electrodes immersed in suspensions of semiconductor particles.<sup>11–13</sup>

The first observation of the photoelectric effect at a metal–electrolyte interface is attributed to Becquerel, who in 1839 noted an electric current between two electrodes immersed in dilute acid solution when one of the electrodes was illuminated with light.<sup>14</sup> Following his observation, this effect was extensively studied and finally demonstrated to result from photoemission process (reviewed in ref 15). The concept was postulated as early as 1965 by Barker et al. who proved that at

certain electrode potentials and photon energies the observed photocurrent arises from photoelectron emission from the metal into the electrolyte solution.<sup>16</sup> Prior to his work, Berg attributed experimentally observed photocurrent at a mercury electrode to the absorption of light by the metal and production of “hot electrons” causing an increase of the electron transfer rate to the solute in the solution.<sup>17</sup> Heyrovsky invoked the concept of photodecomposition of surface charge transfer complexes formed between a metal and a solvent or solute.<sup>18</sup> The absorption of light by these complexes resulted in bond rupture and electron transfer either to the metal or to the adsorbate, depending upon whether the latter functions as an electron donor or an electron acceptor, respectively. Both of these mechanisms are feasible and, at different experimental conditions, can contribute to varying extents to the observed photocurrent. However, the fundamental photoemission process is the direct ejection of an electron into the solution and does not depend on the presence of photoactive species. Ejected electrons undergo rapid thermalization and hydration in solution. The hydrated electron may then react with species in solution (scavengers) or, if none are present, return to the electrode thereby reducing the net photocurrent to zero.

From the dependence of the photocurrent on photon energy and electrode potential, Barker noted that the experimental results did not fit the model developed for photoemission into a vacuum.<sup>16</sup> The presence of the electrical double layer in a condensed medium has a strong influence on the photoemission process. A new quantum mechanical theory was required to describe the photoemission phenomena at metal/electrolyte interfaces. Based on the method of threshold approximation, a so-called “2/5 law” was developed by Brodsky and Gurevich.<sup>19,20</sup> The “2/5 law” has been widely accepted for determining the relationship between the applied potential and the photoemission current.

The effects of the surface roughness on the photoemission have been addressed in several studies. In 1974, Sass et al. demonstrated that the photocurrent for proton reduction at roughened silver electrodes increased by approximately 100 fold over that at smooth Ag surface.<sup>21</sup> The dependence of the

\* To whom all correspondence should be addressed. E-mail: gchumak@iastate.edu. Phone: (515) 294-1066. Fax: (515) 294-0105.

<sup>†</sup> Iowa State University.

<sup>‡</sup> Chinese Academy of Sciences.

photoemission upon photon energy was found to correlate with the surface plasmon absorption in silver. Corrigan and Weaver studied laser-induced electron transfer at metal surfaces for Co(III) and Cr(II) amine complexes.<sup>22</sup> A substantial enhancement of the photocurrent was obtained after electrochemical roughening of silver and gold surfaces. More recently, Kostecki and Augustynski have observed strong cathodic photocurrents for silver electrodes immersed in saturated CO<sub>2</sub> solutions.<sup>23,24</sup> The maximum of the photocurrent also corresponded to the peak of the plasmon resonance in silver.

In the present study, the excitation of surface-plasmon resonances on the surface of electrochemically roughened silver electrode was used to enhance electroreduction of nitrite. It is demonstrated that the photoinduced electroreduction occurred via photoemission of electrons from the metal with subsequent capturing by the electron acceptor. Ammonia was identified as one of the final products in this reaction.

### Experimental Methods

Electrochemical measurements were carried out in a conventional three-electrode cell. A platinum wire served as the auxiliary electrode. A saturated calomel electrode (SCE) was used as the reference electrode. All potentials are reported with respect to the SCE. Working electrodes were constructed from a polycrystalline silver wire that was sealed into glass tubing with Torr Seal (Varian Associates, Palo Alto, CA) epoxy resin. The surface area of the electrodes was ca. 0.09 cm<sup>2</sup>. Before each experiment, the electrode surface was polished in sequence with aqueous suspensions of 5, 0.3, and 0.05  $\mu\text{m}$  alumina until a shiny, mirrorlike finish was obtained. The electrodes were cleaned by sonication three times (total 30 min) in Milli-Q water.

The silver surface was electrochemically roughened using double-potential step oxidation–reduction cycles performed with a custom-built potentiostat/integrator. The supporting electrolyte was 0.1 M Na<sub>2</sub>SO<sub>4</sub>. All solutions were purged with nitrogen gas for 15 min prior to each experiment. Three cycles of the following sequence were performed: the potential was initially stepped to +0.55 V, at which point 25 mC/cm<sup>2</sup> of charge was allowed to pass, and then the potential was stepped to –0.60 V until the current reached a minimum. The electrochemical roughening increased the surface area of the electrode from 0.09 to 0.15 cm<sup>2</sup> as determined by underpotential lead deposition.

Cyclic voltammetric measurements were performed at room temperature with a model 173 potentiostat/galvanostat connected to a model 175 universal programmer (Princeton Applied Research). The cyclic voltammograms (CVs) were plotted on an X–Y recorder. The scan rate was 10 mV/s in all of the experiments.

The working electrode was irradiated with 362, 413, 647, 457, 476, 488, 496, and 514 nm light using Kr<sup>+</sup> (Coherent, Innova 100) and an Ar<sup>+</sup> (Coherent, Innova 200) lasers. The light was focused to a 2 mm spot on the electrode surface. The power was measured with model 210 (Coherent) power meter. Unless otherwise stated, the laser power was 100 mW in all of the experiments.

In the bulk electrolysis experiments, the electrode potential was maintained at –1.0 V. The surface was irradiated continuously and the solution was stirred. The concentration of NH<sub>3</sub> formed during the photoelectrolysis was determined by the Nessler method.<sup>25</sup>

### Results and Discussion

**Effect of Electrode Material and Surface Treatment.** The effect of irradiation on the electrochemical reduction of the

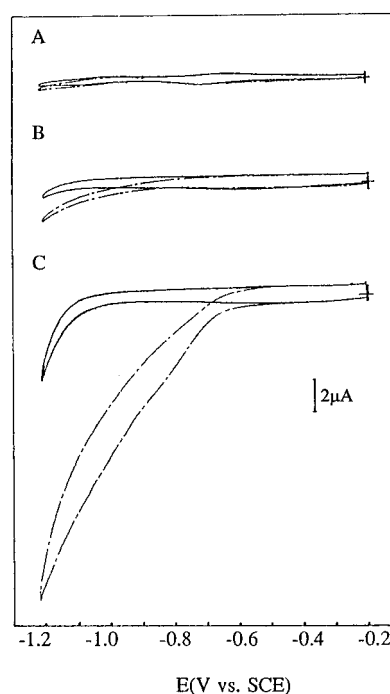


**Figure 1.** Cyclic voltammograms of 1 mM NaNO<sub>2</sub> in 0.1 M Na<sub>2</sub>SO<sub>4</sub> solution at the (A) Hg, (B) polished Ag, and (C) roughened Ag electrodes: (solid curve) in dark; (dashed curve) with 413 nm irradiation.

nitrite (1 mM NaNO<sub>2</sub> in the 0.1 M Na<sub>2</sub>SO<sub>4</sub> solution, pH = 7) at different electrodes is shown in Figure 1. Cathodic currents measured in the dark and under irradiation were compared for different electrodes. The comparison was performed at –1.0 V where there was almost no electrochemical nor photoelectrochemical evolution of hydrogen. In the case of the mercury electrode, very little difference (less than –0.1  $\mu\text{A}$ ) can be noted between CVs measured in the dark and in the light (Figure 1A). A somewhat greater photocurrent (ca. –0.4  $\mu\text{A}$ ) was observed at the polished silver surface (Figure 1B). The roughened silver electrode, in contrast, exhibited a large increase (approximately 26-fold, from ca. –0.4 to –10.7  $\mu\text{A}$ ) in cathodic current during illumination (Figure 1C). This increase cannot be simply attributed to the small (ca. 1.5-fold) increase in the surface area resulting from the roughening. Moreover, the onset potential of the current was also shifted positively by approximately 400 mV from –1.0 to –0.6 V under illumination (Figure 1C). These facts indicate that the photocurrent at the roughened electrode is enhanced due to the excitation of plasmon resonances in nanoscale metal structures generated during the roughening procedure.

**Effect of Excitation Wavelength on the Photoelectrochemical Response.** Cyclic voltammograms measured in 1 mM NaNO<sub>2</sub> and 0.1 M Na<sub>2</sub>SO<sub>4</sub> solution in the dark and under irradiation with a series of excitation wavelengths are shown in Figure 2. Curve a depicts the dark current for the potential scan from –0.2 to –1.2 V. The successive curves b–h were obtained with laser irradiation using 647, 514, 496, 488, 476, 457, and 413 nm wavelengths, respectively. Two important features should be noted: the photocurrent increases with photon energy and the onset potential for the reduction of nitrite shifts positively as the photon energy is increased. The overall shapes of curves a–g are very similar, but curve h (413 nm excitation) has a distinct shoulder near –0.85 V and a relatively larger photocurrent in the potential region between –0.8 and –1.0 V. The shoulder is even more pronounced at higher excitation

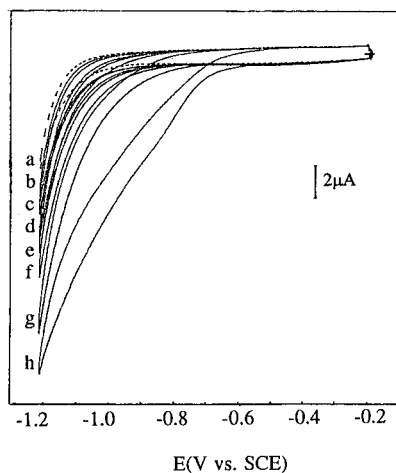


**Figure 2.** Excitation wavelength dependence of cyclic voltammograms of 1 mM  $\text{NaNO}_2$  in 0.1 M  $\text{Na}_2\text{SO}_4$  solution at the roughened Ag electrode: (a) dark; (b) 647; (c) 514; (d) 496; (e) 488; (f) 476; (g) 457; (h) 413 nm.

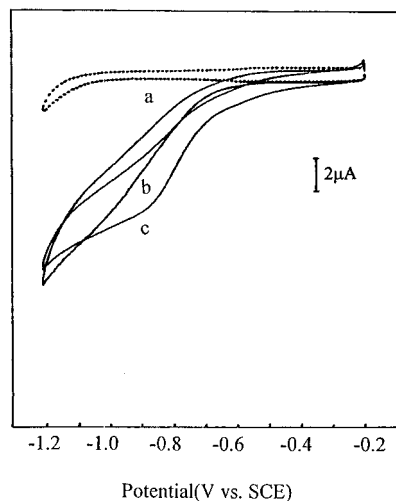


**Figure 3.** Excitation wavelength dependence of cyclic voltammograms of 1 mM  $\text{NaNO}_2$  in 0.1 M  $\text{Na}_2\text{SO}_4$  solution at the roughened Ag electrode: (a) dark; (b) 413 nm; (c) 363.8 nm.

energy (363.8 nm) and appears shifted to more positive potentials (Figure 3). Two peaks in the potential scan under irradiation suggest the presence of two photoinduced electrochemical processes that are “hidden” in an inaccessible negative region without irradiation.

The dependence of the photocurrent at  $-1.0$  V on the excitation wavelength is plotted in Figure 4. Although, this “action spectrum” is not of sufficiently high resolution to determine accurately the maximum in the curve, it is clear that the photocurrent increases rapidly in the spectral region from 500 to 400 nm and decreases below ca. 400 nm. The data, therefore, indicate a resonance behavior of the photocurrent, corresponding to the plasmon resonance absorption in silver.

The possibility that the photocurrent at a roughened silver electrode may result from a photoemission process in which nitrite functions as a scavenger of hydrated electrons is considered next. The dependence of the photocurrent on photon energy and applied potential is well-characterized for the photoemission process from metals into a vacuum.<sup>26</sup> However, this is not an appropriate model for metals in contact with electrolytes, as shown in the study of Barker et al.<sup>16</sup> In the case of the photoemission into a vacuum, the photocurrent is known to depend quadratically on the difference between the energy

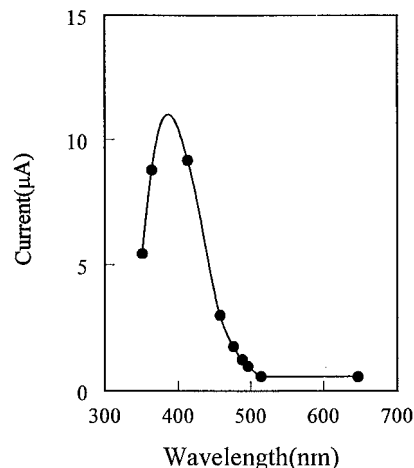


**Figure 4.** Excitation wavelength dependence of photocurrent at  $-1.0$  V for nitrite reduction at the roughened Ag electrode. Data obtained from Figures 2 and 3.

of the excitation photon ( $\hbar\omega$ ) and the threshold photon energy ( $\hbar\omega_0$ ),

$$I \approx (\hbar\omega - \hbar\omega_0)^2 \quad (1)$$

This is known as Fowler’s parabolic law for the photocurrent, where the threshold photon energy is equal to the work function of the metal. In the case of the photoemission into an electrolyte solution, the theoretical description by Brodsky and Gurevich<sup>19</sup> predicts the “5/2 law”

$$I \approx (\hbar\omega - \hbar\omega_0(E))^{5/2} \quad (2)$$

where the threshold photon energy is now dependent upon the electrode potential  $E$ . Thus, the two distinct features of photoemission into an electrolyte solution include the 5/2 power dependence and the shift in the threshold photon energy with the electrode potential

$$\hbar\omega_0 = \hbar\omega_0(E_0) + e(E - E_0) \quad (3)$$

where  $E_0$  is the potential of zero charge. Data obtained for the photoreduction of nitrite ion will next be analyzed in terms of the above two predictions.

The plot of the photocurrent raised to the 0.4 power versus potential measured at  $-1.0$  V is shown in Figure 5. In the case of 1 mM  $\text{NaNO}_2$  in a 0.1 M  $\text{Na}_2\text{SO}_4$  solution, a nonlinear behavior can be observed near the onset potential (Figure 5, curve a). A similar phenomenon was also reported by Pleskov et al., who claimed that the nonlinearity is related to the low concentration of electrolyte or electron acceptor in the double layer.<sup>27</sup> The “5/2 law”, which is based on the threshold approximation, is only valid for concentrated electrolytes where the potential drop between metal and solution is confined to the dense part of the double layer. As can be seen in the case of 0.5 M  $\text{NaNO}_2$  in the 1 M  $\text{Na}_2\text{SO}_4$  solution, the data fit the expected linear relationship quite well (Figure 5, curve b).

The plot of the onset potential versus photon energy is shown in Figure 6. The onset potential was determined from Figure 2 as the potential at which the current started to flow in the cathodic scan. The relationship is linear, in agreement with eq 3; however, the slope is ca.  $-2.0$  instead of  $-1.0$  expected for concentrated acceptor solutions.<sup>28</sup> The larger slope could result from low acceptor concentration.<sup>15</sup>

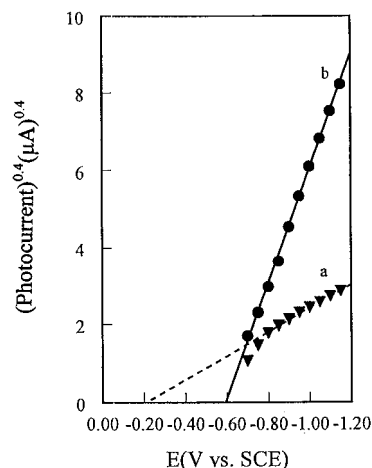


**Figure 5.** Potential dependence of photocurrent for nitrite reduction at roughened Ag electrodes in (a) 1 mM  $\text{NaNO}_2$  + 0.1 M  $\text{Na}_2\text{SO}_4$  solution and (b) 0.5 M  $\text{NaNO}_2$  + 1 M  $\text{Na}_2\text{SO}_4$  solution.

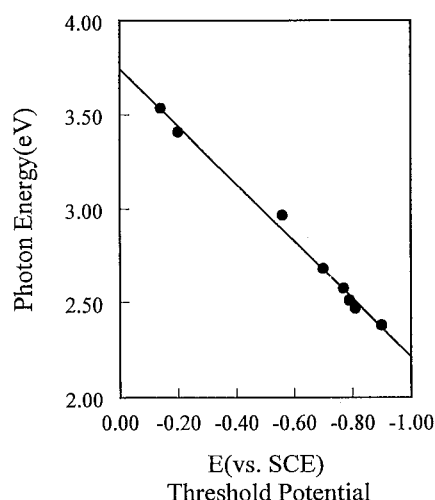


**Figure 6.** Photon energy dependence of onset potential. Data obtained from Figures 2 and 3.

The photoelectrochemical response as a function of nitrite concentration in the range between 0.5 and 10 mM exhibits nonlinear behavior (Figure 7, insert). According to the model in which hydrated electrons are captured by electron scavengers, it is expected that this response should follow square root dependence at low concentrations and reach saturation at high concentrations.<sup>19</sup> Indeed, the corresponding plot in Figure 8 confirms this model for the photoreduction of nitrite at electrochemically roughened silver surface. The square root dependence reflects the fact that not all photoemitted electrons were captured by nitrite ions; some electrons returned to the electrode. This back current is affected by nitrite concentration. The dependence of the photocurrent on the incident laser power follows linear behavior which is characteristic of a one-photon process<sup>29</sup> and is expected for the power used in these experiments (Figure 9).

The time evolution of the photocurrent in a quiescent, 1 mM nitrite solution is shown in Figure 10. When the electrode was first irradiated, the photocurrent reached the initial value of 24  $\mu\text{A}$ . After ca. 40 s of continues irradiation, the photocurrent decayed exponentially to its steady state value of 12  $\mu\text{A}$ . It is important to mention that this current remained nearly constant as long as the concentration of nitrite ions remained unchanged, indicating little or no poisoning of the electrode surface by reaction intermediates or products. Electrolysis experiments at

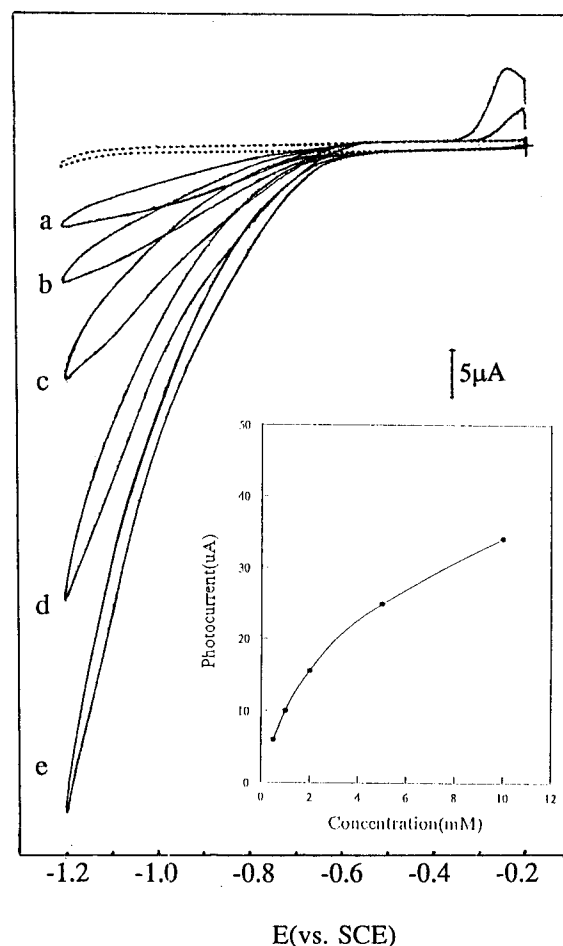


**Figure 7.** Cyclic voltammograms of  $\text{NaNO}_2$  with different concentration at the roughened Ag electrode with 413 nm irradiation: (dashed curve) dark; (a) 0.5; (b) 1; (c) 2; (d) 5; (e) 10 mM. Insert: plot of photocurrent at  $-1.0$  V versus concentration.

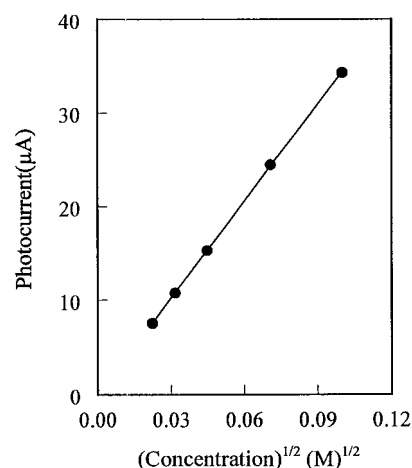


**Figure 8.** Plot of photocurrent as a function of  $C^{1/2}$ . Data obtained from Figure 7.

the controlled potential were further performed under the irradiation with 413 nm light, and ammonia was detected as one of the products.

On the basis of the experimental results, possible mechanisms for the photoelectrochemical reduction of nitrite at a roughened silver electrode are proposed. Photogenerated hydrated electrons  $e^-$  (aq) are captured by nitrite to form  $\text{NO}_2^{2-}$ , which undergoes hydrolysis. Following this initial photochemical step, several electrochemical reactions take place:

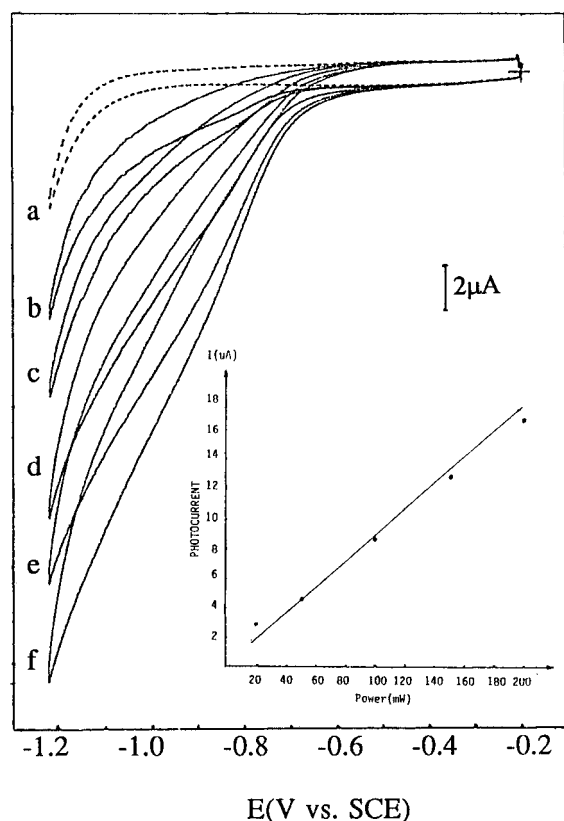


**Figure 9.** Photoresponse of 1 mM NaNO<sub>2</sub> in 0.1 M Na<sub>2</sub>SO<sub>4</sub> solution at -1.0 V at the roughened Ag electrode with 413 nm irradiation.

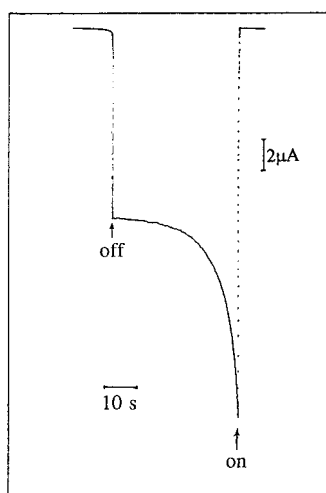
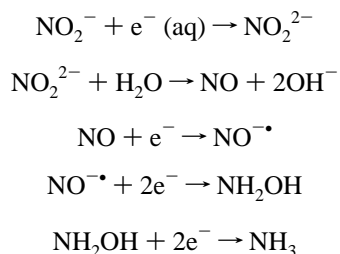


**Figure 10.** Power dependence of cyclic voltammograms of 1 mM NaNO<sub>2</sub> in 0.1 M Na<sub>2</sub>SO<sub>4</sub> solution at the roughened Ag electrode with 413 nm irradiation. Inset: plot of photocurrent at -1.0 V versus power of irradiation.



It is important to emphasize that the measured current is the sum of the photocurrent and the current due to subsequent electrochemical reactions. This issue must be taken in to account

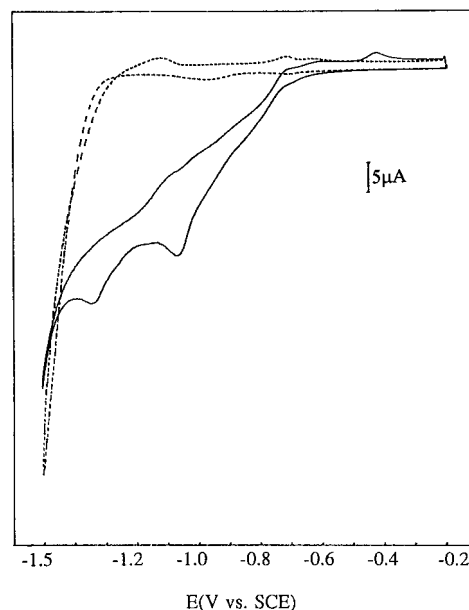
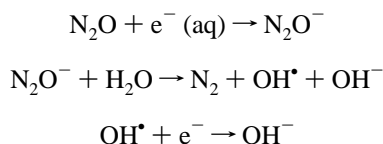


**Figure 11.** Cyclic voltammograms of 1 mM NaNO<sub>2</sub> in 0.1 M NaOH solution at the roughened Ag electrode: (dashed curve) in dark; (solid curve) with 413 nm irradiation.

when determining the photoelectrochemical efficiency. In the proposed mechanism, the total number of the electrons crossing the interface is six and only one electron is photogenerated.

Even though no measurements of nitrogen gas were performed in this study, its formation could also take place. As the concentration of NO<sup>•</sup> product in the diffusion layer increases, the dimeric species (N<sub>2</sub>O<sub>2</sub>)<sup>2-</sup> can be formed with further decomposition into N<sub>2</sub>O.<sup>29</sup> Nitrous oxide can then react with the hydrated electron and undergo the following reactions:



Three photoelectrons among a total of six are required for the reduction of 2NO<sub>2</sub><sup>-</sup> to nitrogen gas N<sub>2</sub> according to this scheme. Finally, any electrochemical reaction following the photochemical step can “utilize” hydrated electrons as well. This fact complicates even more the exact determination of the number of photoelectrons that contribute to the measured photocurrent making calculations of the photoefficiency difficult. Nevertheless, we estimated the quantum efficiency of about 0.04% for nitrite photoreduction on the electrochemically roughened silver surface. The estimate is based exclusively on the assumption that only one photoelectron is captured.

**Effect of pH.** The pH of the solution strongly affects the reduction potential of nitrite, as demonstrated for a number of different electrodes.<sup>30–33</sup> For the silver electrode, Cattarin<sup>6</sup> reported that the nitrite reduction in the 1 M NaOH begins in the potential region of hydrogen evolution, ca. -1.4 V. The product formed was identified as ammonia. Our results obtained in the dark in 1 mM NaNO<sub>2</sub> and 0.1 M NaOH solution are consistent with that report (Figure 11, dashed curve). However, when irradiated with 413 nm light, the onset potential for the reduction was shifted to -0.6 V (Figure 11, solid curve). Comparing to that at neutral pH (Figure 1, C), two new features at -1.08 and -1.35 V appeared in the cathodic scan. These features could represent the reduction of different intermediates,



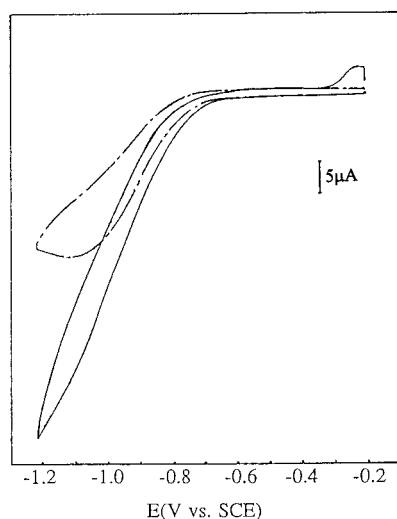


**Figure 12.** Cyclic voltammograms of 1 mM  $\text{NaNO}_3$  in 0.1 M  $\text{Na}_2\text{SO}_4$  solution at the roughened Ag electrode: (dashed curve) in dark; (solid curve) with 413 nm irradiation.

reduction potentials of which are shifted to more positive values in alkaline pH. It should be noted that under irradiation the onset potentials for the nitrite reduction were the same at  $-0.6$  V in both neutral and alkaline solutions, thereby indicating that the photoemission process is essentially independent of pH.

**Reduction of Nitrate.** A photoelectrochemical response was also observed in the solution of nitrate (Figure 12). Nitrate can be electrochemically reduced to nitrite without irradiation via a two-electron step process (Figure 12, dashed curve). The reduction peak at  $-1.1$  V reflects a large overpotential that is required for this reaction because of the rapid reoxidation of the high energy  $\text{NO}_3^{2-}$  intermediate ion.<sup>29</sup> Since no light is required to convert nitrate to nitrite, the observed photocurrent was attributed mainly to the photoelectrochemical reduction of nitrite according to mechanisms described above. The limiting step in the overall reaction is the electrochemical reduction of  $\text{NO}_3^-$  to  $\text{NO}_2^-$  that occurs at the potentials more negative than the onset potential for the photoelectrochemical reduction of  $\text{NO}_2^-$ . For this reason, no dependence of the onset potential on irradiation is expected. Indeed, the reduction current under irradiation (Figure 12, solid curve) increased ca. twice relative to the dark current with no or very little shift in the onset potential. A small shift that can be assumed in Figure 12 is due to the fact that the reduction of nitrate to nitrite can also occur by capturing hydrated electrons generated by photoemission. This reaction will compete with the electrochemical reduction of nitrate, and depending upon relative contributions of these two pathways, more or less shift in the onset potential will be observed.

## Conclusion

Enhanced photoelectrochemical reduction of nitrite and nitrate was observed on roughened silver surfaces compared to "smooth" silver and mercury when irradiated with light in the blue-green spectral region. In the case of nitrite, the irradiation resulted in an increase of the reduction current along with a shift of the onset potential, as was determined from the comparison of CVs measured in the dark and under illumination conditions. It was determined that the photocurrent is proportional to the  $5/2$  power of the applied potential and to the square root of the nitrite concentration in the solution. On the basis of these data as well as the linear relationship between the onset potential and photon energy, it was concluded that the photo-

electrochemical reduction involves a photoemission process from the metal followed by capture of the hydrated electrons by nitrite. The dependence of the photocurrent on irradiation power and wavelength suggests a one-photon process that involves the excitation of plasmon resonances in nanoscale metal structures on the roughened silver surface. Electrolysis experiments at the controlled potential and under irradiation revealed ammonia as one of the products. Two mechanisms are proposed for nitrite reduction. In the case of nitrate reduction, it is suggested that nitrate was first reduced to nitrite via a two-electron electrochemical step followed by photoelectrochemical reduction of nitrite.

**Acknowledgment.** Research at Ames Laboratory is supported by the Division of Chemical Sciences, Office of Basic Energy Sciences, U.S. Department of Energy. Ames Laboratory is operated for the U.S. Department of Energy by Iowa State University under Contract W-7405-Eng-82.

## References and Notes

- Genders, J. D.; Hartsough, D.; Hobbs, D. T. *J. Appl. Electrochem.* **1996**, 26, 1.
- Coleman, D. H.; White, R. E.; Hobbs, D. T. *J. Electrochem. Soc.* **1995**, 142, 1152.
- Van de Moedijk, C. G. M. *Chem. Ind.* **1984**, 18, 189.
- Strehlitz, B.; Grundig, B.; Schumacher, W. *Anal. Chem.* **1996**, 68, 807.
- Wu, Q.; Storrier, G. D.; Pariente, F. *Anal. Chem.* **1997**, 69, 4856.
- Cattarin, S. J. *J. Appl. Electrochem.* **1992**, 22, 1077.
- Nishimura, K.; Machida, K.; Enyo, M. *Electrochim. Acta* **1991**, 36, 877.
- Xing, X.-K.; Scherson, D. A. *J. Electroanal. Chem.* **1986**, 199, 485-488.
- Taniguchi, I.; Nakashima, N.; Matsushita, K.; Yasukouchi, K. *J. Electroanal. Chem.* **1987**, 224, 199-209.
- Fung, C.-S.; Wong, K.-Y. *J. Electroanal. Chem.* **1996**, 401, 263.
- Halman, M.; Tobin, J.; Zuckerman, K. *J. Electroanal. Chem.* **1986**, 209, 405.
- Baldwin, R. P.; Perone, S. P. *J. Electrochem. Soc.* **1976**, 123, 1647.
- Babenko, S. D.; Benderskii, V. A.; Zolotovskii, Y. A. M.; Krivenko, A. G. *J. Electroanal. Chem.* **1977**, 76, 347.
- Becquerel, E. *Compt. Rend.* **1839**, 9, 145.
- Brodsky, A. M.; Pleskov, Y. V. *Surface Sci.* **1972**, 2, 1.
- Barker, G. C.; Gardner, A. W.; Sammon, D. C. *J. Electrochem. Soc.* **1966**, 113, 1183.
- Berg, H. *Rev. Polarogr.* **1963**, 11, 29.
- Heyrovsky, M.; Norrish, R. G. W. *Nature* **1965**, 200, 1356.
- Brodsky, A. M.; Gurevich, Y. Y. *Sov. Phys. JETP* **1968**, 54, 213.
- Brodsky, A. M. In *Excess Electrons in Dielectric Media*; Ferradini, C., Jay-Gerin, J.-P., Eds.; CRC Press: Boca Raton, 1991; Chapter 11.
- Sass, J. K.; Sen, R. K.; Meyer, E.; Gerischer, H. *Surface Sci.* **1974**, 44, 515.
- Corrigan, D. S.; Weaver, M. J. *J. Electroanal. Chem.* **1987**, 228, 265.
- Kostecki, R.; Augustynski, J. *J. Appl. Phys.* **1995**, 77, 4701.
- Fedurco, M.; Shklover; Augustynski, J. *J. Phys. Chem.* **1997**, 101, 5158.
- Marczenko, Z. In *Separation and Spectrophotometric Determination of Elements*; Masson, M., Ed.; Ellis Harwood Limited: Chichester, England, 1986; Chapter 35.
- Fowler, R. H. *Phys. Rev.* **1931**, 38, 45.
- Pleskov, Y. V.; Rotenberg, Z. A. *J. Electroanal. Chem.* **1969**, 20, 1.
- Gurevich, Y. Y.; Pleskov, Y. V.; Rotenberg, Z. A. In *Photoelectrochemistry*; Wroblowa, H. S., Conway, B. E., Eds.; Consultants Bureau: New York, 1980; Chapter 4.
- Benderskii, V. A.; Benderskii, A. V. *Laser Electrochemistry of Intermediates*; CRC Press: New York, 1995; Chapter 7.
- Ehman, D. L.; Sawyer, D. T. *J. Electroanal. Chem.* **1968**, 16, 541.
- Vicente, F.; Garcia-Jareño, J. J.; Tamarit, R.; Cervilla, A.; Domenech, A. *Electrochim. Acta* **1995**, 40, 1121.
- Reuben, C.; Galun, E.; Cohen, H.; Tenne, R.; Kalish, R.; Muraki, Y.; Hashimoto, K.; Fujishima, A.; Butler, J. M.; Lévy-Clément, C. *J. Electroanal. Chem.* **1995**, 396, 233.
- Fung, C.-S.; Wong, K.-Y. *J. Electroanal. Chem.* **1996**, 401, 263.